MSJ Experimental Translational Clinical

Original Research Paper

Early imaging predictors of longer term multiple sclerosis risk and severity in acute optic neuritis

Multiple Sclerosis Journal—Experimental, Translational and Clinical

July-September 2019, 1–9

DOI: 10.1177/2055217319863122

Sanuji Gajamange, Jim Stankovich, Gary Egan, Trevor Kilpatrick, Helmut Butzkueven, Joanne Fielding, Anneke van der Walt and Scott Kolbe

Abstract

Background: Biomarkers are urgently required for predicting the likely progression of multiple sclerosis (MS) at the earliest stages of the disease to aid in personalised therapy.

Objective: We aimed to examine early brain volumetric and microstructural changes and retinal nerve fibre layer thinning as predictors of longer term MS severity in patients with clinically isolated syndromes (CIS).

Methods: Lesion metrics, brain and regional atrophy, diffusion fractional anisotropy and retinal nerve fibre layer thickness were prospectively assessed in 36 patients with CIS over the first 12 months after presentation and compared with clinical outcomes at longer term follow-up [median (IQR) = 8.5 (7.8–8.9) years].

Results: In total, 25 (69%) patients converted to MS and had greater baseline lesion volume ($p = 0.008$) and number ($p = 0.03$)than CIS patients. Over the initial 12 months, new lesions ($p = 0.0001$), retinal nerve fibre layer thinning ($p = 0.04$) and ventricular enlargement ($p = 0.03$) were greater in MS than CIS patients. In MS patients, final Expanded Disability Status Scale score correlated with retinal nerve fibre layer thinning over the first 12 months ($\rho = -0.67$, $p = 0.001$).

Conclusions: Additional to lesion metrics, early measurements of fractional anisotropy and retinal nerve fibre layer thinning are informative about longer term clinical outcomes in CIS.

Keywords: Multiple sclerosis, MRI, OCT, neurodegeneration, disease severity, inflammation

Date received: 25 March 2019; accepted: 11 June 2019

Introduction

There is an urgent need for biomarkers that can provide prognostic information regarding disease progression in people with multiple sclerosis (MS). Quantitative assessments of the number and volume of focal brain lesions using magnetic resonance imaging (MRI) are used for monitoring the neuroinflammatory component of MS. However, MS is also associated with significant degeneration of axons and neurons, commonly termed neurodegeneration, which leads to irreversible and progressive neurological impairment.[1] Since neurodegenerative processes are thought to be initiated by inflammatory processes, early inflammatory burden can, to a degree, predict longer term clinical outcomes.[2] However, lesion metrics fail to fully account for MS progression,[3] and in later disease stages neurodegeneration occurs in the absence of concomitant inflammation.[4] Therefore, there is considerable interest in evaluating surrogate markers of neurodegeneration for use in monitoring and predicting disease progression in MS, and as trial endpoints for therapies with putative neuroprotective effects.[5] Such markers must also respond at the earliest disease stages such as clinically isolated syndromes (CIS), when the greatest therapeutic window exists.

Neurodegeneration can be measured using a variety of imaging techniques. Loss of brain tissue (atrophy) can be measured using high resolution MRI scans and has been shown to correlate with disability.[6] Studies in CIS cohorts have demonstrated that

Correspondence to:
Scott Kolbe,
Department of Neuroscience, Central Clinical School, Monash University, Australia.
scott.kolbe@monash.edu.

Sanuji Gajamange, Department of Medicine and Radiology, University of Melbourne, Australia

Jim Stankovich, Department of Neuroscience, Central Clinical School, Monash University, Australia

Gary Egan, Monash Biomedical Imaging, Monash University, Australia

Trevor Kilpatrick, The Florey Institute of

Neuroscience and Mental Health, Australia

Helmut Butzkueven, **Joanne Fielding**, **Anneke van der Walt**, **Scott Kolbe**, Department of Neuroscience, Central Clinical School, Monash University, Australia

ventricular enlargement and brain atrophy (global brain and grey matter) worsen over time, and correlate with clinical outcome.[7–9] Diffusion tensor imaging (DTI) changes indicate damage to tissue microstructure both within MS lesions and diffusely throughout normal-appearing white matter.[10] A longitudinal DTI study in patients with established MS showed progressive changes in the corpus callosum that could be reliably measured over relatively short time periods (<12 months).[11] Retinal nerve fibre layer (RNFL) thickness can be measured using optical coherence tomography (OCT) and has been proposed as potential early marker of neurodegeneration.[12–14] RNFL thickness decreases over time,[15] and despite being a retinal measure specifically, it correlates with axonal damage in the visual pathways of the brain[16] and whole brain atrophy.[17]

In this study we prospectively assessed brain MRI (lesions, volumes and DTI) and OCT (RNFL thickness) variables over the first 12 months following acute presentation with clinically isolated unilateral optic neuritis (ON). All patients had at least one brain lesion (>3 mm^3), thus placing them at high risk for developing MS.[18] Patients were followed-up clinically for up to 10 years in order to assess: (a) differences in baseline and early change in MRI and OCT variables between patients subsequently diagnosed with MS and those who remained CIS, and (b) in those patients who did convert to MS, the early MRI and OCT variables that predicted subsequent time to second relapse, number of relapses, and disability accumulation over the follow-up period. We hypothesised that in addition to lesion metrics, measures relating to neurodegeneration would also significantly predict the severity of MS.

Methods

Subjects and testing

Forty-five patients presenting with acute unilateral ON were recruited from the Royal Victorian Eye and Ear Hospital, Australia. Seven patients were excluded from the study: five did not exhibit any cerebral T2-hyperintense lesions on MRI, placing them at low risk of conversion to MS; one had incomplete data; and one had recurrent ON. Two patients withdrew prior to 12 months follow-up. The remaining 36 patients underwent baseline MRI testing within 48 h of initial presentation, and prior to administration of methylprednisolone. Patients returned for MRI scanning 12 months after initial recruitment. At both visits, a full neurological examination was performed, which included disease severity assessment with the Expanded Disability Severity Score (EDSS)[19] and OCT. Clinical histories of all patients were assessed up to 10 years after initial presentation [median (IQR) = 8.5 (7.8–8.9) years; follow-up durations for all patients are included in the Appendix] either through examination of hospital records, or, in cases where patients had not presented to clinics, through phone contact. Of the 36 patients, 25 were confirmed to have been diagnosed with MS according to the 2010 McDonald criteria at follow-up which includes evidence for dissemination in time from MRI scans without a concomitant neurological relapse. For patients who had converted to MS, the timing and number of subsequent relapses was recorded, as well as the most recently recorded EDSS. Eleven patients were started on disease-modifying treatment 6 months from baseline, and 15 patients by 12 months (Appendix).

Healthy comparison MRI data were acquired as part of a longitudinal observational study of patients with Huntington's disease[20] using an identical MRI protocol on the same MRI system to that used for this study. A sample of 23 healthy controls matched for age and sex was used for comparisons with patients. Control participants had no reported history of neurological disease were scanned twice 18 months apart with an identical MRI protocol to that used for patients.

This study was conducted in accordance with the Declaration of Helsinki and was approved by the Human Research Ethics Committees of the Royal Victorian Eye and Ear Hospital and the Royal Melbourne Hospital. All study participants provided voluntary, written consent.

Optical coherence tomography

Time-domain OCT was performed using an OCT-3 scanner (Stratus^{TM}, software version 3.0, Carl Zeiss Meditec Inc.) using the fast RNFL protocol. The acquisition consists of three circular 3.4mm diameter scans centred on the optic disc. Scans with signal strength of <7 were discarded. Average whole and temporal quadrant RNFL thickness values were calculated for the clinically unaffected eyes at baseline, 1, 3, 6 and 12 months. Annual change in RNFL thickness was calculated by fitting a line of best fit using the least squares method. Missing data were calculated by taking the average measure from visits before and after. When baseline measures were unavailable, the constant from the line of best fit was used. Outliers were defined as being above or

below twice the median absolute deviation and removed from the analysis.

MRI acquisition and lesion assessments

Image acquisition was performed using a Siemens Trio 3T MRI system (Siemens, Erlangen, Germany) with a 32 channel head coil. The following sequences were performed at baseline and 12-month follow-up:

1. T1-weighted MPRAGE images (repetition time = 1900 ms, echo time = 2.63 ms; flip angle = 9°; inversion time = 900 ms; voxel size = $0.8 \times 0.8 \times 0.8\,mm^3$),
2. 3D FLAIR scan (repetition time = 6000 ms, echo time = 418 ms; inversion time = 2100 ms; echo train length = 145 ms; flip angle = 120°; voxel size = $0.9 \times 0.9 \times 0.9\,mm^3$),
3. 2D spin-echo diffusion-weighted echo planar imaging (repetition time = 8200 ms, echo time = 89 ms; 10 non-diffusion-weighted images with b = 0 s/mm^2 and 60 diffusion-weighted images at b = 1200 s/mm^2; voxel size = $2 \times 2 \times 2\,mm^3$).

At baseline only patients also underwent a second T1-weighted MPRAGE scan (repetition time = 1680 ms, echo time = 2.37 ms; flip angle = 9°; inversion time = 900 ms; voxel size = $0.9 \times 0.9 \times 0.9\,mm^3$) after intravenous injection with 0.01 mmol/kg dimegluine gadopenate [single dose gadolinium] to identify enhancing lesions. Lesion numbers for FLAIR and gadolinium scans were counted by a neuroradiologist. FLAIR lesion volume at baseline and 12 month follow-up was calculated using a semi-automated thresholding technique[21] and checked by a neuroradiologist.

Brain volumetric analyses

Two analysis packages were used for volumetric analysis: FSL (v5.0.6) SIENA/SIENAX and FreeSurfer (v5.1.0) in order to take advantage of their relative strengths.

FSL provides tools for cross-sectional (SIENAX) and longitudinal (SIENA) volumetric brain measurements.[22,23] SIENAX involves brain extraction, affine registration of the skull to MNI152 space to obtain a volumetric scaling factor for head size normalisation. Tissue segmentation with partial volume estimation was performed to calculate normalised grey, white and total brain volume. SIENA calculates longitudinal brain volume changes (ventricle and brain volume). SIENA performs brain extraction on two brain images, which are then aligned to each other, and resampled into the space midway between the two. The average boundary displacement between the two images was calculated and expressed as an annualised percentage change.

FreeSurfer was used to calculate volumes for cortical and subcortical brain structures using the longitudinal pipeline (v1.75.2.2).[24] An unbiased within-subject template space and image was created using robust inverse consistent registration. Skull stripping, Talairach transformation and atlas registration and spherical surface maps and parcellation were performed with mutual information within-subject template. Ventricle size, corpus callosum, cortical grey and white matter, and subcortical grey matter (sum of thalamus, caudate, accumbens, putamen, globus pallidus and ventral diencephalon volumes) volumes were calculated. Longitudinal volume changes were expressed as an annualised percentage change.

Diffusion Tensor Imaging

Diffusion-weighted MRI data were realigned and eddy-current distortion corrected (FLIRT, FSL). Diffusion tensor images were calculated with the FSL diffusion toolkit and normalised to MNI152 space using a diffusion tensor image registration toolkit (DTI-TK v2.3.3). A study-specific DTI template was generated in MNI152 space using a previously described method.[25] Briefly, each subject's DTI data were linearly registered to the ICBM DTI-81 template. The resulting images were averaged to create a first-pass template. Each subject's DTI data were then linearly and nonlinearly registered to the first-pass template, and the resulting registered DTI data were averaged to create a second-pass template. This procedure was repeated to create the final third-pass template. Next, each subject's DTI data were normalised to the final template with an affine and nonlinear registration. Fractional anisotropy (FA) maps were estimated from the normalised DTI data. The Johns Hopkins University White Matter Atlas was used to identify large association tracts: corpus callosum (CC), corticospinal tract (CST), inferior longitudinal fasciculus (ILF) and cingulum (Cing). Optic radiation DTI for this cohort has been previously reported[26] and compared with affected optic nerve damage which was not the focus of this study. Each white matter tract was transformed from MNI to the final diffusion template space and the average FA value was calculated for each white matter tract for each subject. In order to determine the total microstructural damage to each white matter tract, mean tract FA was

calculated from both normal-appearing and lesional white matter together.

Statistical analyses

For all statistical tests, normality was assessed using Kolmogorov–Smirnov tests. For non-normally distributed data, non-parametric tests were performed only if transformation of the data (logarithmic or polynomial) did not normalise the distribution. Patients were stratified into MS and CIS according to their last recorded clinical status. To account for multiple comparisons significance was set at $p<0.05$ after false discovery rate correction using the Benjamini–Hochberg Procedure.[27]

Baseline volumetric measures and DTI were compared between healthy controls, CIS and MS using one-way analysis of variance (ANOVA) for normally distributed data and Kruskal–Wallis one-way ANOVA for non-normal data. Student's *t*-tests or Mann–Whitney *U*-tests were performed to compare baseline RNFL thickness and lesion volume between the CIS and MS patient cohorts. Longitudinal analyses were performed to examine differences in the annualised percentage change of the volumetric measurements, FA and RNFL thickness using one-way ANOVA (parametric or Kruskal–Wallis depending on data normality).

A Cox proportional hazards survival analysis was performed on each measure separately (baseline and longitudinal volumes, DTI and RNFL thickness) to identify measures associated with time to second clinical relapse. A backwards stepwise selection procedure was applied, starting with the significant measures from the above analyses, to fit a multivariable model and determine the strongest predictor/s.

In order to identify early factors that predict longer term disease severity in patients who did convert to MS, partial Spearman correlation analyses, controlled for age and treatment duration, were performed between clinical outcomes (final EDSS or total number of relapses) and baseline and longitudinal changes in lesion load, volumetric measures, DTI and RNFL thickness.

Results

Table 1 summarises the disease characteristics for all subjects. No group differences were detected for age or sex. At baseline, cerebral gadolinium enhancing lesions were identified in 7/25 (28%) of patients who converted to MS. No patients who did not convert to MS exhibited cerebral gadolinium enhancing lesions at baseline.

The number of newly appearing lesions ($p=0.0001$) over the first 12 months after presentation were greater in MS patients compared with CIS. Baseline FA in the CC ($F_{(2,54)}=6.04$, $p=0.004$) (Figure 1(a)) and CST ($F_{(2,54)}=7.07$, $p=0.002$) (Figure 1(b)) differed significantly across the groups. Post-hoc comparisons indicated that changes in CC FA differed between MS and controls ($p=0.003$), and CST FA differed between CIS and controls ($p=0.028$), and between MS and controls ($p=0.002$).

Survival analysis was performed to determine the MRI and OCT parameters associated with the time to second relapse. Age, gender, baseline and longitudinal measures of brain and optic nerve injury were examined individually. Baseline variables that were associated with an increase in rate of a second relapse at baseline included lesion volume [hazard ratio (HR) $=1.23$, $p=0.01$], lesion number ($HR=1.03$, $p=0.002$) and average RNFL thickness ($HR=1.03$, $p=0.04$). Changes in following variables over the first 12 months were also associated with an increase in rate of a second relapse: number of new appearing lesions ($HR=2.27$, $p=0.00003$), corpus callosum atrophy ($HR=1.28$, $p=0.02$), ventricular enlargement ($HR=1.07$, $p=0.04$), cerebral white matter atrophy ($HR=1.41$, $p=0.05$), and loss of FA in the CC ($HR=1.14$, $p=0.02$). After applying a backward stepwise selection procedure, only newly appearing lesion number remained significant [$HR(95\%\ CI)=2.40(1.56,\ 3.65)$, $p=0.00005$)]. Trend effects were observed for annualised CC atrophy ($HR=1.16$, $p=0.10$) and baseline average RNFL thickness loss ($HR=1.02$, $p=0.08$). The duration of disease-modifying treatment exposure did not have a significant influence on the time to second relapse.

Table 2 summarises the relationship between clinical outcome in patients who converted to MS, and baseline and longitudinal changes in lesion, volumetric, DTI and OCT variables. In MS patients, final EDSS correlated negatively with RNFL thinning ($p=0.001$, Figure 2). No variables predicted number of relapses.

Discussion

This study involved acute MRI and OCT markers of inflammation and neurodegeneration in CIS patients at acute presentation and after 12 months and longer

Table 1. Demographics and disease characteristics up to 10 years follow-up. Baseline and annualised longitudinal measures of volumetric atrophy and microstructural abnormalities.

	Controls (n=23)	CIS (n=11)	CDMS (n=25)	p
Age[a]	37.3 ± 6.5	39.1 ± 6.9	35.0 ± 6.5	0.313
Sex	15F, 8M	7F, 4M	18F, 7M	0.835
Baseline				
Gd^+ Lesions (no. of patients)		0 (0%)	7 (28%)	–
FLAIR Lesion Count[d]	–	7.27 ± 9.90	21.68 ± 24.04	0.008
FLAIR Lesion vol. (mm^3)[c]	–	225.1 ± 347.5	2111.4 ± 6959.8	0.030
RNFL thickness (non-ON eye, μm)				
Average[c]	–	110 ± 10	101 ± 16	0.087
Temporal[d]	–	73 ± 8	68 ± 14	0.261
SIENAX ($\times 10^3\ mm^3$)				
Normalised GM volume[a]	831.4 ± 45.1	829.4 ± 60.9	847.0 ± 59.2	0.529
Normalised WM volume[a]	760.6 ± 47.8	768.9 ± 36.0	755.9 ± 30.8	0.658
Normalised total brain volume[a]	1592.0 ± 83.9	1598.2 ± 81.3	1602.8 ± 75.6	0.895
FreeSurfer ($\times 10^3\ mm^3$)				
Ventricle[a]	9.0 ± 3.1	10.8 ± 3.3	9.9 ± 4.1	0.394
CC[a]	2.3 ± 0.3	2.3 ± 0.4	2.1 ± 0.3	0.181
Supratentorial WM[a]	312 ± 18	309 ± 23	302 ± 16	0.161
Cortical GM[a]	406 ± 22	400 ± 20	406 ± 23	0.740
Subcortical GM[a]	31 ± 3	31 ± 2	30 ± 2	0.195
DTI – FA[e]				
CC[a]	**0.58 ± 0.02**	**0.57 ± 0.02**	**0.56 ± 0.02**	**0.004[f]**
CST[a]	**0.48 ± 0.02**	**0.47 ± 0.02**	**0.47 ± 0.02**	**0.002[f]**
ILF[b]	0.42 ± 0.02	0.41 ± 0.02	0.40 ± 0.02	0.069
Cing[a]	0.40 ± 0.03	0.39 ± 0.04	0.38 ± 0.02	0.115
Longitudinal (annual % change)				
New lesions (no.)[d]	**–**	**0**	**1.40 ± 1.16**	**0.0001[f]**
RNFL thickness (non-ON eye)				
Average[c]	–	–0.5 ± 5.2	–0.1 ± 4.3	0.791
Temporal[c]	–	6.4 ± 12.5	–2.0 ± 10.4	0.044
SIENA				
Ventricle[a]	0.82 ± 2.04	–0.44 ± 2.42	3.16 ± 5.71	0.033
Brain[a]	–0.14 ± 0.25	0.003 ± 0.49	–0.26 ± 0.50	0.219
FreeSurfer				
CC[a]	0.11 ± 1.89	0.79 ± 0.86	–0.86 ± 2.56	0.072
Cortical WM[b]	0.27 ± 1.24	0.43 ± 1.02	–0.55 ± 1.10	0.051
Cortical GM[b]	–0.81 ± 1.78	–0.18 ± 1.31	–0.25 ± 1.92	0.694
Subcortical GM[b]	–0.20 ± 1.11	–0.10 ± 0.82	–0.70 ± 1.39	0.155
DTI – FA[e]				
CC[b]	–0.12 ± 2.46	–2.70 ± 5.26	1.19 ± 3.49	0.078
CST[a]	–1.47 ± 3.08	–0.46 ± 4.10	0.10 ± 3.68	0.328
ILF[b]	0.41 ± 3.50	–2.36 ± 7.91	1.04 ± 5.03	0.248
Cing[b]	–0.82 ± 5.92	–4.27 ± 6.45	1.19 ± 8.57	0.053

ON: optic neuritis; CC: corpus callosum, WM: white matter, GM: grey matter, CST: corticospinal tract; ILF: inferior longitudinal fasciculus; Cing: cingulum. [a]One-way ANOVA; [b]Kruskal–Wallis one-way ANOVA; [c]Independent-samples t-test; [d]Independent-samples median test; [e]DTI analysis included MS n=24; [f]significant at FDR-corrected $p<0.05$.

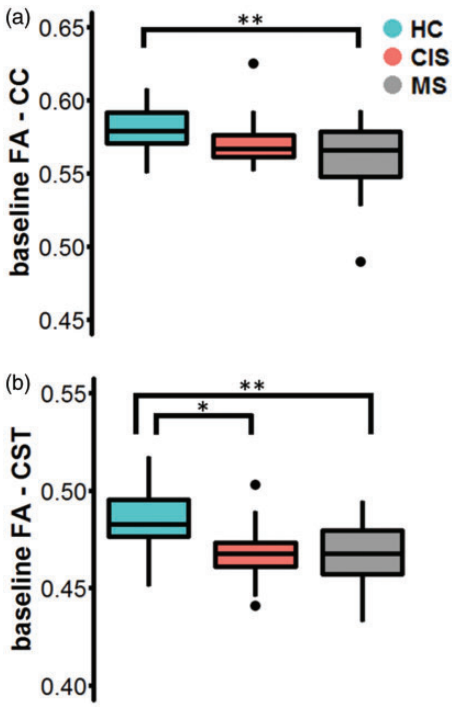

Figure 1. Boxplots illustrating the baseline FA measures within the (A) corpus callosum (CC) and (B) cortico-spinal tract (CST). HC: healthy control; CIS: clinically isolated syndrome; MS: multiple sclerosis *$p<0.05$, **$p<0.01$.

term (<10 years) clinical follow-up to identify early predictors of longer term disease severity. Lesion activity at baseline and its accumulative change over 12 months were greater in MS than CIS patients. Multivariate Cox regression showed that the number of newly appearing lesion was the only significant predictor of rate of second relapse, demonstrating that clinical relapses are strongly associated with early MRI inflammatory activity. This confirms previous studies reporting that baseline lesion load is significantly greater in patients who develop MS.[8,28–30] Furthermore, the rate of developing clinically definite MS in our study (69%) was similar to that observed by ON treatment trials (56–72%).[31,32]

A key aim of this study was to assess whether early measurements using imaging techniques sensitive to neurodegeneration (brain volumetry, DTI and OCT) could provide additional information relevant to disease progression. Compared with controls, MS patients exhibited significantly reduced FA in the CC and CST at baseline , and compared with CIS, MS patients exhibited greater ventricular enlargement, and greater temporal RNFL thinning in the non-ON eye. Greater CC and total white matter atrophy, and ventricular enlargement over the first year was associated with the rate of second clinical relapse. However, these variables lost significance in the competing analysis with lesion metrics, demonstrating that the main driver of relapses is neuroinflammatory activity. Unexpectedly, the FA change in MS patients was positive whereas a negative change was observed in CIS. This finding could reflect the interplay between changes in axonal density that drive FA changes and macroscopic tissue loss that drives volume change. New diffusion MRI techniques have been recently developed to simultaneously account for these processes,[33] but further methodological testing and validation is required before the methods can be used in clinical settings.

We observed a trend towards reduction in RNFL thickness at baseline and significant RNFL thinning over the subsequent 12 months in the non-ON eye in MS patients compared with CIS. Furthermore, early RNFL thinning significantly predicted final EDSS. Together, these results suggest that RNFL thinning is a useful marker of disease severity in patients who have been identified as at high risk for converting to MS made by lesion assessments. Our results are supported by several studies demonstrating correlations between progressive RNFL thinning and disability progression.[13,34,35] Although we measured RNFL thickness from non-ON eyes, the visual system is highly integrated and it is possible that ON-related damage to the affected eye could affect the non-ON eye due to trans-synaptic degeneration via the lateral geniculate nucleus. Retrograde axonal degeneration within the optic radiations has been previously documented in patients after acute ON.[36] We observed a positive correlation between the number of clinical relapses and brain volume change over the first 12 months in patients with MS. This was an unexpected finding and could relate to ongoing inflammatory activity that is associated with oedema and swelling.

Several limitations should be considered when interpreting the results of this study. First, treatment of inflammation in previously untreated disease can exaggerate the measurement of atrophy during early follow-up, a phenomenon known as pseudoatrophy. However, it should be noted that in this study brain volume measures did not yield significant results for between-group or correlation analyses. Second, we utilised time-domain OCT rather than the more recently developed spectral-domain OCT. Time-domain OCT provides lower resolution, is more susceptible to misalignment errors during setup of the scan, making longitudinal assessments less reproducible, and provides only very limited

Table 2. Relationship between clinical outcome and measures of brain injury in MS patients. Spearman partial correlation coefficients between clinical measures (EDSS and number of relapses) and, baseline and annualised longitudinal change (volumetric and microstructural).

	EDSS		Number of relapses	
	ρ	p	ρ	p
Baseline				
Lesion (no.)	0.07	0.78	0.20	0.42
Lesion vol. (ml)	–0.02	0.92	–0.03	0.91
RNFLT (non-ON eye, μm)				
Average	0.10	0.68	–0.17	0.50
Temporal	0.02	0.90	–0.42	0.07
SIENAX ($\times 10^{-6}$ mm^3)				
Grey	0.02	0.93	0.26	0.29
White	0.23	0.32	0.24	0.34
Brain	0.11	0.65	0.34	0.17
FreeSurfer				
Ventricle ($\times 10^{-3}$)	0.21	0.37	0.05	0.84
CC ($\times 10^{-3}$)	–0.04	0.85	0.07	0.77
Cerebral WM	–0.07	0.76	-0.13	0.61
Cortical GM	–0.24	0.30	0.08	0.74
Subcortical GM	0.28	0.22	0.29	0.23
DTI – FA				
CC	–0.30	0.23	–0.03	0.92
CST	0.12	0.63	0.02	0.94
ILF	–0.22	0.36	0.28	0.28
Cing	–0.33	0.17	–0.02	0.94
Longitudinal (annual % change)				
New lesions (no.)	0.21	0.36	0.11	0.66
RNFLT (non-ON eye)				
Average	**–0.67**	**0.001**[a]	–0.22	0.37
Temporal	0.22	0.35	–0.11	0.65
SIENA				
Ventricle	–0.21	0.37	–0.25	0.31
Brain	0.03	0.88	0.17	0.48
FreeSurfer				
CC	–0.17	0.48	–0.05	0.85
Cerebral WM	–0.21	0.37	0.45	0.06
Cortical GM	0.26	0.25	–0.10	0.70
Subcortical GM	0.12	0.62	0.57	0.01
DTI – FA				
CC	–0.03	0.91	0.32	0.19
CST	–0.56	0.01	0.02	0.92
ILF	–0.37	0.11	0.05	0.83
Cing	–0.35	0.14	0.05	0.86

ON: optic neuritis; CC: corpus callosum, WM: white matter, GM: grey matter, CST: corticospinal tract; ILF: inferior longitudinal fasciculus; Cing: cingulum. [a]significant at FDR-corrected $p<0.05$

ability to measure the volume of individual retinal layers. Despite these limitations, a recent meta-analysis of spectral-domain OCT studies for MS demonstrated that RNFL thinning is the most robust measure for assessing neurodegeneration in MS.[37] Third, the rate of recruitment of patients for this study was slow (two per month), resulting in relatively small group sizes after stratification. This is a common limitation of studies recruiting patients with acute ON who are facing the potential

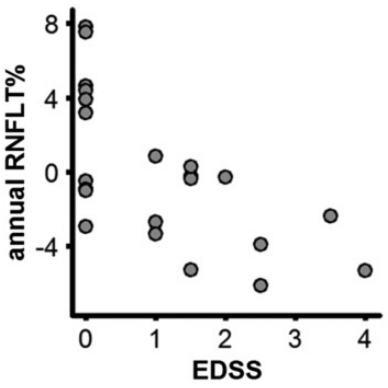

Figure 2. Scatterplot showing the relationship between the rate of retinal nerve fibre layer thinning over the first 12 months after acute optic neuritis and EDSS at long-term follow-up.

diagnosis with a life-long chronic disease. Finally, it should be noted that correction for multiple comparisons was not performed in this study due to the relatively low sample size. To overcome the difficulties with prospective recruitment of patients with acute ON, future studies could consider integrating OCT and DTI assessments into standard clinical follow-up.

Conclusions

Our results demonstrated that early inflammatory activity and RNFL thinning over the 12 months after initial presentation provide complementary information about disease progression in CIS patients. Novel prognostic algorithms that integrate standard radiological assessments of lesions, together with newer imaging assessments that are sensitive to neurodegenerative changes, could improve the prediction of longer term clinical outcomes in MS and should be explored in larger cohorts to inform clinical practice.

Conflict of Interests

The author(s) declared no potential conflicts of interest with respect to the research, authorship, and/or publication of this article.

Funding

The author(s) disclosed receipt of the following financial support for the research, authorship, and/or publication of this article: This research was supported by the National MS Society (Grant RG4211A4/2#) and the National Health and Medical Research Council of Australia (Grant APP1009757, APP1054147), Multiple Sclerosis Research Australia (Postgraduate Scholarship #14-088). The funders had no role in study design, data collection and analysis, decision to publish, or preparation of the manuscript.

ORCID iD

Anneke van der Walt https://orcid.org/0000-0002-4278-7003
Scott Kolbe https://orcid.org/0000-0003-4685-1380

Supplemental Material

Supplemental material for this article is available online.

References

1. Trapp BD, Peterson J, Ransohoff RM, et al. Axonal transection in the lesions of multiple sclerosis. *New Engl J Med* 1998; 338: 278–285.
2. Brex PA, Ciccarelli O, O'Riordan JI, et al. A longitudinal study of abnormalities on MRI and disability from multiple sclerosis. *New Engl J Med* 2002; 346: 158–164.
3. Barkhof F, Calabresi PA, Miller DH, et al. Imaging outcomes for neuroprotection and repair in multiple sclerosis trials. *Nat Rev Neurol* 2009; 5: 256.
4. Pérez-Cerdá F, Sánchez-Gómez MV and Matute C. The link of inflammation and neurodegeneration in progressive multiple sclerosis. *Mult Scler Demyelinating Disord* 2016; 1: 9.
5. Tur C, Moccia M, Barkhof F, et al. Assessing treatment outcomes in multiple sclerosis trials and in the clinical setting. *Nat Rev Neurol* 2018; 14: 75.
6. De Stefano N, Airas L, Grigoriadis N, et al. Clinical relevance of brain volume measures in multiple sclerosis. *CNS Drugs* 2014; 28: 147–156.
7. Pérez-Miralles F, Sastre-Garriga J, Tintoré M, et al. Clinical impact of early brain atrophy in clinically isolated syndromes. *Mult Scler J* 2013; 19: 1878–1886.
8. Dalton CM, Brex PA, Jenkins R, et al. Progressive ventricular enlargement in patients with clinically isolated syndromes is associated with the early development of multiple sclerosis. *J Neurol Neurosurg Psychiatry* 2002; 73: 141–147.
9. Raz E, Cercignani M, Sbardella E, et al. Gray- and white-matter changes 1 year after first clinical episode of multiple sclerosis: MR imaging. *Radiology* 2010; 257: 448–454.
10. Basser PJ, Mattiello J and LeBihan D. MR diffusion tensor spectroscopy and imaging. *Biophys J* 1994; 66: 259–267.
11. Harrison DM, Caffo BS, Shiee N, et al. Longitudinal changes in diffusion tensor-based quantitative MRI in multiple sclerosis. *Neurology* 2011; 76: 179–186.
12. Alonso R, Gonzalez-Moron D and Garcea O. Optical coherence tomography as a biomarker of neurodegeneration in multiple sclerosis: A review. *Mult Scler Relat Disord* 2018; 22: 77–82.
13. Britze J and Frederiksen JL. Optical coherence tomography in multiple sclerosis. *Eye* 2018; 32: 884–888.
14. Pierro L, Gagliardi M, Iuliano L, et al. Retinal nerve fiber layer thickness reproducibility using seven

different OCT instruments. *Invest Ophthalmol Vis Sci* 2012; 53: 5912–5920.
15. Herrero R, Garcia-Martin E, Almarcegui C, et al. Progressive degeneration of the retinal nerve fiber layer in patients with multiple sclerosis. *Invest Ophthalmol Vis Sci* 2012; 53: 8344–8349.
16. Kolbe S, Marriott M, van der Walt A, et al. Diffusion tensor imaging correlates of visual impairment in multiple sclerosis and chronic optic neuritis. *Invest Ophthalmol Vis Sci* 2012; 53: 825–832.
17. Saidha S, Al-Louzi O, Ratchford JN, et al. Optical coherence tomography reflects brain atrophy in multiple sclerosis: A four-year study. *Ann Neurol* 2015; 78: 801–813.
18. Volpe NJ. The optic neuritis treatment trial: A definitive answer and profound impact with unexpected results. *Arch Ophthalmol* 2008; 126: 996–999.
19. Kurtzke JF. Rating neurologic impairment in multiple sclerosis: An Expanded Disability Status Scale (EDSS). *Neurology* 1983; 33: 1444.
20. Dominguez DJ, Egan GF, Gray MA, et al. Multi-modal neuroimaging in premanifest and early Huntington's disease: 18 month longitudinal data from the IMAGE-HD study. *PLoS One* 2013; 8: e74131.
21. Rorden C and Brett M. Stereotaxic display of brain lesions. *Behav Neurol* 2000; 12.
22. Smith SM, Rao A, De Stefano N, et al. Longitudinal and cross-sectional analysis of atrophy in Alzheimer's disease: Cross-validation of BSI, SIENA and SIENAX. *Neuroimage* 2007; 36: 1200–1206.
23. Cover KS, van Schijndel RA, van Dijk BW, et al. Assessing the reproducibility of the SienaX and Siena brain atrophy measures using the ADNI back-to-back MP-RAGE MRI scans. *Psychiatry Res* 2011; 193: 182–190.
24. Reuter M, Schmansky NJ, Rosas HD, et al. Within-subject template estimation for unbiased longitudinal image analysis. *Neuroimage* 2012; 61: 1402–1418.
25. Kolbe SC, Kilpatrick TJ, Mitchell PJ, et al. Inhibitory saccadic dysfunction is associated with cerebellar injury in multiple sclerosis. *Hum Brain Mapp* 2014; 35: 2310–2319.
26. Kolbe S, van der Walt A, Butzkueven H, et al. Serial diffusion tensor imaging of the optic radiations after acute optic neuritis. *J Ophthalmol* 2016; 2016: 6.
27. Benjamini Y and Hochberg Y. Controlling the false discovery rate – a practical and powerful approach to multiple testing. *J R Stat Soc B* 1995; 57: 289–300.
28. Kolasa M, Hakulinen U, Helminen M, et al. Longitudinal assessment of clinically isolated syndrome with diffusion tensor imaging and volumetric MRI. *Clin Imaging* 2015; 39: 207–212.
29. Tintore M, Rovira A, Rio J, et al. Baseline MRI predicts future attacks and disability in clinically isolated syndromes. *Neurology* 2006; 67: 968–972.
30. Kalincik T, Vaneckova M, Tyblova M, et al. Volumetric MRI markers and predictors of disease activity in early multiple sclerosis: A longitudinal cohort study. *PLoS ONE* 2012; 7: e50101.
31. Optic Neuritis Study Group. The 5-year risk of MS after optic neuritis - Experience of the optic neuritis treatment trial. *Neurology* 1997; 49: 1404–1413.
32. Optic Neuritis Study Group. Multiple sclerosis risk after optic neuritis: Final optic neuritis treatment trial follow-up. *Arch Neurol* 2008; 65: 727–732.
33. Gajamange S, Raffelt D, Dhollander T, et al. Fibre-specific white matter changes in multiple sclerosis patients with optic neuritis. *NeuroImage Clin* 2018; 17: 60–68.
34. Talman LS, Bisker ER, Sackel DJ, et al. Longitudinal study of vision and retinal nerve fiber layer thickness in multiple sclerosis. *Ann Neurol* 2010; 67: 749–760.
35. Saidha S, Sotirchos ES, Oh J, et al. Relationships between retinal axonal and neuronal measures and global central nervous system pathology in multiple sclerosis. *JAMA Neurol* 2013; 70: 34–43.
36. Kolbe S, Bajraszewski C, Chapman C, et al. Diffusion tensor imaging of the optic radiations after optic neuritis. *Hum Brain Mapp* 2012; 33: 2047–2061.
37. Petzold A, Balcer LJ, Calabresi PA, et al. Retinal layer segmentation in multiple sclerosis: A systematic review and meta-analysis. *Lancet Neurol* 2017; 16: 797–812.

Appendix

Table Clinical summary for each patient. Follow-up direction is considered as the time between the first clinical presentation and the latest time of follow-up. DMT: disease-modifying treatment

Patient	Final diagnosis	Time to conversion (months)	Follow-up duration (months)	DMT and commenced time (months)
001	MS	12	103.1	
002	CIS	–	20	
003	MS	0	111.5	Glatiramer acetate at 6 mo.
004	MS	0	106.4	Interferon beta-1b at 6 mo.
005	Excluded (normal brain MRI)	–	–	–

(continued)

Table Continued

Patient	Final diagnosis	Time to conversion (months)	Follow-up duration (months)	DMT and commenced time (months)
006	CIS	–	93.4	
007	MS	6	105.9	Interferon beta-1a at 6 mo.
008	MS	6	19	
009	CIS	–	114.8	
010	Withdrew prior to follow-up	–	–	–
011	CIS	–	114.5	
013	CIS	–	114.4	
014	Excluded (normal brain MRI)	–	–	–
015	MS	0	41	Glatiramer acetate at 6 mo.
016	Withdrew prior to follow-up	–	–	–
017	MS	59.5	59.5	
018	MS	6	102.3	Interferon beta-1a at 6 mo.
019	Excluded (incomplete dataset)	–	–	–
020	MS	0	103.2	Glatiramer acetate at 6 mo.
021	MS	12	98.3	
022	Excluded (normal brain MRI)	–	–	–
023	MS	6	128.5	Interferon beta-1b at 12 mo.
024	CIS	–	109.6	
025	MS	6	109.2	Interferon beta-1a at 6 mo.
026	MS	74.5	74.5	
027	MS	36	103.5	
028	MS	12	100.9	Interferon beta-1a at 6 mo.
029	CIS	–	66.9	
030	MS	36	100.2	
031	MS	12	97	Glatiramer acetate at 12 mo.
032	MS	12	107	
033	MS	36	107.2	Interferon beta-1b at 6 mo.
034	CIS	–	107	
035	Excluded (normal brain MRI)	–	–	–
036	MS	6	94.7	Interferon beta-1a at 12 mo.
037	CIS	–	28	
038	MS	100.2	100.2	
039	MS		25	Interferon beta-1a at 12 mo.
040	MS		103	Natalizumab at 6 mo.
041	CIS	–	99	
042	CIS	–	96.4	
043	MS	0	111.6	Interferon beta-1a at 6 mo.
044	MS	6	95	
045	Excluded (normal brain MRI)	–	–	–
046	Excluded (recurrent ON)	–	–	–